Talanta 104 (2013) 193–197

Contents lists available at SciVerse ScienceDirect

Talanta

journal homepage: www.elsevier.com/locate/talanta

Short communication

QCM immunoassay for recombinant cysteine peptidase: A potential protein biomarker for diagnosis of citrus canker

André S. Afonso [a,c], Bianca F. Zanetti [b], Adelita C. Santiago [b], Flavio Henrique-Silva [b], Luiz H.C. Mattoso [c], Ronaldo C. Faria [a,*]

[a] Departamento de Química, Universidade Federal de São Carlos, CP 676, 13565-905, São Carlos, SP, Brazil
[b] Departamento de Genética e Evolução, Universidade Federal de São Carlos, CP 676, 13565-905, São Carlos, SP, Brazil
[c] EMBRAPA Instrumentação Agropecuária, CP 741, 13560-970, São Carlos, SP, Brazil

ARTICLE INFO

Article history:
Received 25 September 2012
Received in revised form
1 November 2012
Accepted 3 November 2012
Available online 13 November 2012

Keywords:
Biomarker
Citrus canker
Citrus disease
Cysteine peptidase
Immunosensor
QCM

ABSTRACT

Citrus canker is one of the most important agricultural citrus diseases worldwide. It is caused by *Xanthomonas citri* subsp. *citri* (*Xcc*) bacterium that infects leaves and the fruits produce a cysteine peptidase (CPXaC), which makes it a potential target for the development of effective and rapid detection methods for citrus canker. We report here the studies on the development of piezoelectric immunoassay for CPXaC using a polyclonal antibody against CPXaC (anti-CPXaC). Three different strategies for covalent immobilization of anti-CPXaC on gold surfaces were evaluated by monitoring the frequency (Δf) and energy dissipation (ΔD) variation in real time when 64.5×10^{-8} mol L^{-1} CPXaC was added. Anti-CPXaC immobilized with 11-mercaptoundecanoic acid (MUA) showed the best relation between the frequency and dissipation factor variation, and strong values for the kinetic and equilibrium binding constant were obtained. The immunosensor showed a detection limit of 13.0 nmol L^{-1} with excellent specificity, showing no response for different proteins that include another cysteine peptidase that is used as a target to detect *Xylella fastidiosa* bacterium, responsible for another important citrus disease. These results provide good perspectives for the use of CPXaC as a new biomarker for citrus canker.

© 2012 Elsevier B.V. All rights reserved.

1. Introduction

Citrus canker is one of the high economic impact diseases affecting citrus species worldwide. It is caused by *Xanthomonas citri* subsp. *citri* (*Xcc*), a gram-negative bacterium and is characterized by conspicuous, erumpent lesions on leaves, stems, and fruits [1]. The disease can cause defoliation, blemished fruit, premature fruit drop, and tree decline [2]. There is no cure or treatment for citrus canker, so once the infected trees are detected, the surrounding symptomless trees must be destroyed to avoid further infections that could result in high economic losses [3]. The disease exists in more than 30 countries, therefore the efforts to control and eradicate the infected areas and to maintain canker-free areas are economically important for the citrus market [4]. Conventional methods as polymerase chain reaction (PCR), spectral information divergence classification methods, and laser induced fluorescence spectroscopy have been used for citrus canker detection; however they are time consuming, labor intensive, expensive and require expertise [4–6]. A realizable expectation to prevent and control the new infections could be offered by the early detection of citrus canker, coupled with strategies to prevent its further spread. Thus, the use of immunosensors for the detection of protein biomarkers emerges as an alternative assay for simple, accurate and cost effective citrus canker diagnosis.

The dissipation factor of a quartz crystal microbalance (QCM-D) is a known high-sensitive technique that quantifies and monitors in real-time mass changes on the surface of a piezoelectric quartz crystal [7]. QCM-D also has the capability to monitor the energy dissipation (*D*-factor) that can be correlated with the films' viscoelasticity property. In this case, if a soft layer is deposited on a crystal surface the shift in the resonance frequency does not necessarily correspond only to the amount of mass adsorbed, but also to the viscoelasticity variation on the layer [8]. Thus, the *D*-factor could be used to compare different tailored surfaces for the development of sensors. So the best strategy for sensor design is related not only to the maximum resonance frequency variation but also to the lowest variation in the dissipation factor (*D*) for a same amount of analyte added to the sensors [9–12].

It has recently been demonstrated that phytopathogenic bacteria includes the genus *Xanthomonas* [13] that uses a cysteine peptidase to change plant physiology and which is related to

* Corresponding author. Tel.: +55 16 3351 8084; fax: +55 16 3351 8053.
E-mail address: rcfaria@ufscar.br (R.C. Faria).

0039-9140/$ - see front matter © 2012 Elsevier B.V. All rights reserved.
http://dx.doi.org/10.1016/j.talanta.2012.11.003

countless relevant biological processes. The cysteine peptidase produced by *Xcc* (CPXaC) is probably involved in the invasion processes of the host, which then makes a potential protein biomarker for the development of effective and rapid diagnosis methods for the detection of citrus canker. In this paper we describe for the first time the development of a label-free QCM-D immunosensor for CPXaC detection using an anti-CPXaC immobilized on a crystal surface using different self-assembled monolayer (SAM) strategies. The piezoelectric immunoassay developed showed high sensitive and selective real-time responses for CPXaC. This approach opens the door to use CPXaC as a potential protein biomarker for simple, low-cost, and fast immunoassay for citrus canker detection.

2. Experimental

The reagents, apparatus, the expression and purification of recombinant cysteine peptidase, polyclonal antibody and the immunosensor construction are described in detail in the supplementary materials. Three anti-CPXaC immobilization procedures on the gold surface of the quartz were evaluated as follows: *Immobilization procedure 1* (IP1): The polyclonal anti-CPXaC was immobilized in 11-mercaptoundecanoic acid (MUA); *Immobilization procedure 2* (IP2): The polyclonal anti-CPXaC was immobilized in a mixture (1:10) of MUA and 6-mercapto-1-hexanol (MHO); *Immobilization procedure 3* (IP3): anti-CPXaC was immobilized using cystamine (Cyst). Fig. 1 shows the immobilization procedures studied (for more details see supplementary materials). All procedures were evaluated based on resonance frequency variation as well as variation in dissipation *D*-factor for antigen–antibody interaction to achieve the best response for CPXaC.

3. Results and discussion

3.1. Anti-CPXaC immobilization on crystal surface

Three different anti-CPXaC immobilization procedures on the crystal surface were evaluated by real-time monitoring of Δf and ΔD variation. For this the modified piezoelectric crystal sensor was inserted into a flow cell, and pH 7.2 phosphate saline (PBS) buffer (0.01 mol L^{-1} phosphate, 0.15 mol L^{-1} NaCl) was pumped, and after the frequency was stabilized, CPXaC in PBS was injected. Fig. 2 shows the variation of the third harmonic resonance frequency and dissipation factor as a function of time for the injection of 64.5×10^{-8} mol L^{-1} CPXaC to three different anti-CPXaC modified crystals. When CPXaC was added, the resonance frequency decreased for all modified crystals due to the antigen–antibody binding process. The largest shift in resonance frequency was observed for crystals modified with MUA/MHO (IP2) and MUA (IP1) and the lowest for IP3 that used Cyst SAM

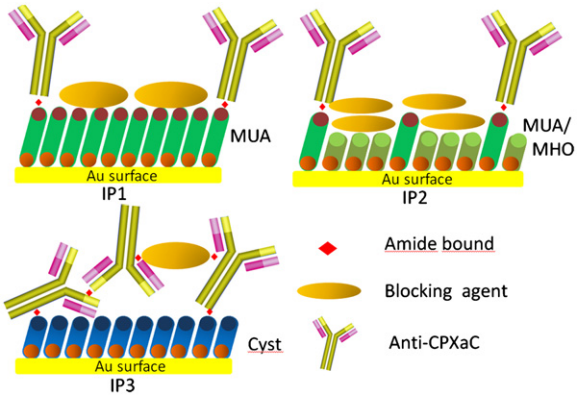

Fig. 1. Schematic showing the procedures IP1, IP2, and IP3 used for anti-CPXaC immobilization on gold surface of the quartz crystal.

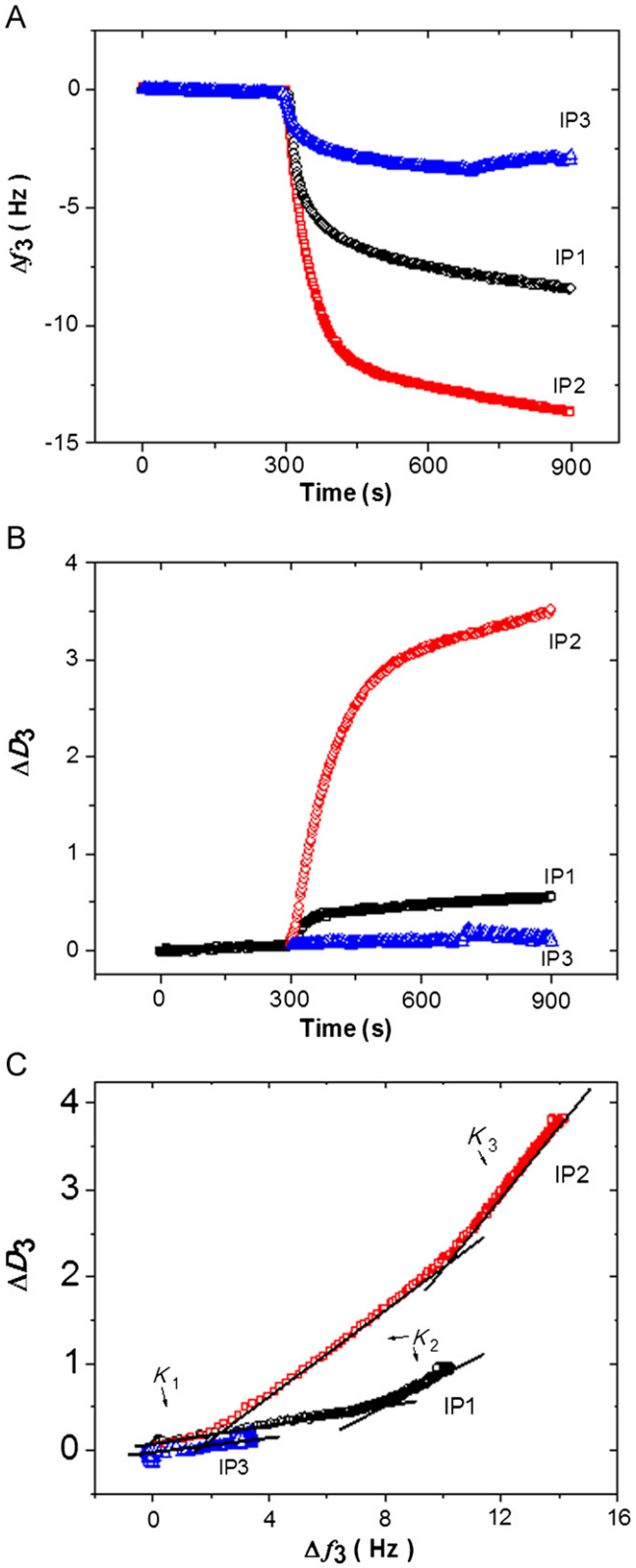

Fig. 2. Real-time variation of Δf (A) and ΔD (B) when 64.5×10^{-8} mol L^{-1} CPXaC was added into QCM-D cell (C) $\Delta D/\Delta f$ plots for added 64.5×10^{-8} mol L^{-1} CPXaC into QCM-D obtained from (A) and (B). Piezoelectric immunosensors were constructed using three different procedures IP1, IP2 and IP3.

and anti-CPXaC. The immobilization using a mixture of MUA and MHO was employed as a way to avoid steric hindrance for the antibody–antigen interaction in the crystal surface in order to improve the binding process [14]. Comparing the immobilization procedures with and without MHO (IP1 and IP2) it was observed (Fig. 2(A)) that the presence of MHO led to the highest Δf, about 70% more than that in the absence of MHO, indicating that thus far the use of a MUA/MHO mixture is a more efficient immobilization procedure for CPXaC binding. The crystal modified by IP3 showed the lowest Δf probably due to the chemical modification of the antibody with EDC/NHS in solution, which can lead to antibody–antibody bonding formation, hence decreasing the number of free paratopes. On the other hand, IP3 showed the lowest ΔD variation when CPXaC was added to the cell. The crystal modified with IP3 presented a ΔD of 0.1×10^{-6}, followed by 0.93×10^{-6} for MUA, and 3.8×10^{-6} for MUA/MHO (Fig. 2(B)). The small variation in the D-factor for the sensor modified with IP3 indicated that the film formed after the binding process is more rigidly coupled to the crystal when compared with MUA/MHO and MUA. The immobilization procedures using MUA/MHO and MUA show a higher variation in ΔD when CPXaC was injected, indicating that the antigen–antibody interaction resulted in a change in the viscoelastic properties of the film [15,16]. Fig. 2(C) presents the ΔD vs Δf plots obtained from the data in Fig. 2(A and B) and the slopes, K_n, indicated different relaxation times during the binding processes [17]. The immunosensors showed distinguishable kinetic processes with three, two and one slopes for MUA/MHO, MUA, and Cyst, respectively, as summarized in Table 1. In all cases K_1 presents small and very similar values, indicating that the kinetic of the antigen–antibody binding is fast, leading to the mass increased of the film; however the film retains its rigidity as confirmed by the tiny variation in D-factor. The sensor developed by the IP3 procedure presents only the K_1 slope, which can be associated to the binding processes with practically no variation in the viscoelastic properties, hence indicating a good correlation between frequency variation and the mass uptake, according to the Sauerbrey equation. However the variation in frequency obtained using IP3 procedure was quite small for analytical purposes. MUA/MHO and MUA immobilization procedures showed small values for $\Delta D/\Delta f$ immediately after the addition of CPXaC; however for MUA/MHO $\Delta D/\Delta f$ change rapidly to high values (K_2) and when the frequency variation reaches about 10 Hz, $\Delta D/\Delta f$ increased again, indicating conformational changes in the antigen–antibody binding process (K_3). Although anti-CPXaC immobilization procedure based on the use of MUA/MHO showed the highest Δf value when CPXaC was added, a large shift in the dissipation factor was observed, indicating that the variation in frequency can be attributed not only to the antigen mass uptake but also to conformational changes and/or water trapped in the film [15–17]. However, the sensor constructed using MUA presents the smallest variation in $\Delta D/\Delta f$ indicating a more rigid and compact layer that can be ascribed to antigen–antibody interaction. Considering our findings, further studies were carried out using IP1 based on MUA. The film obtained by IP1 was characterized by PM-IRRAS and contact angle, more details can be obtained in the SI.

Table 1
Values of $\Delta D/\Delta f$ for the different immobilization procedures obtained from Fig. 2.

	Immobilization procedure		
$\Delta D/\Delta f$ (10^{-6} Hz^{-1})	IP1 (MUA)	IP2 (MUA/MHO)	IP3 (Cyst)
K_1	0.05	0.08	0.07
K_2	0.17	0.28	–
K_3	–	0.41	–

3.2. Immunosensor development

After the best procedure for anti-CPXaC immobilization was determined, the analytical curve was obtained by recording the Δf after adding different CPXaC concentrations into the QCM-D cell, followed by a CPXaC-free PBS injection, Fig. 3(A and B). As can be seen, when the antigen concentration raised, Δf increased and a linear shift was observed in the concentration range studied, exhibiting a limit of detection of 13.0 nmol L^{-1} based on signal-to-noise ratio (S/N) of three, with a correlation coefficient of 0.973. At the same time, variation in D-factor was evaluated after the injection of different concentrations of CPXaC. The lowest ΔD variation means that the film is rigid, thus frequency response can be well described by the Sauerbrey equation [18]. Thus, lower ΔD values we obtained with procedure IP1, suggesting a rigid and compact film in the concentration range used, as shown in

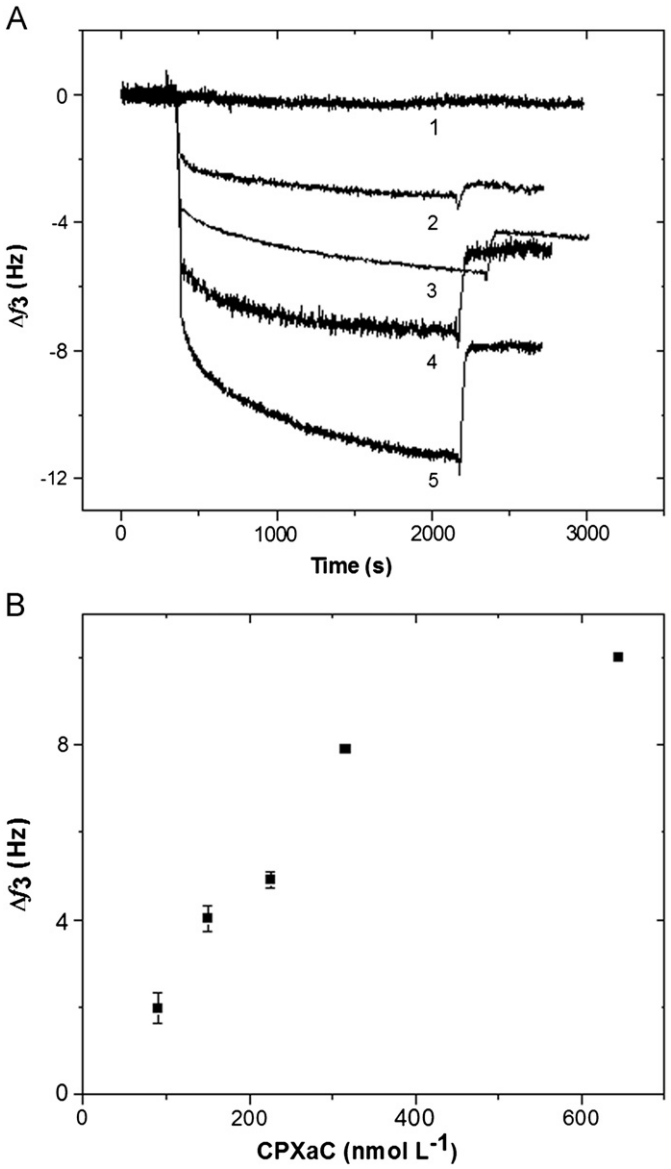

Fig. 3. (A) Real-time curves of frequency variation for different CPXaC concentrations from 0 to 64.5×10^{-8} mol L^{-1} of CPXaC (curves 1–5) injected in continuous flux of PBS buffer pH 7.2. (B) Analytical curve for CPXaC immunosensor.

Table S-1 in supplementary materials. The plot of $\Delta D/\Delta f$ as a function of CPXaC concentration showed low and constant values indicating that the stiffer protein layer was obtained after antigen and antibody (see Fig. S-2 in supplementary materials).

3.3. Kinetics and association equilibrium constants

The determination of affinity constant is important to evaluate the feasibility of the antibody used for biosensor applications. The equilibrium and kinetics constants were evaluated by measuring the shift in frequency when different concentrations of CPXaC were added to the quartz crystal with the immobilized anti-CPXaC using two methods, as previously reported [11,19]: *Method* I: used the variation between initial and final frequency and Langmuir Isotherm model to obtain the association binding constant, K_a, and *Method* II: used the frequency decreasing in real time to obtain the binding and dissociation kinetic constants, k_a and k_d respectively. A detailed description of binding constant calculations is included in the supplementary materials. Table 2 presents the association constants calculated by both procedures, which showed values as high as those observed for other antigen–antibody binding processes [20,21] indicating that anti-CPXaC is a good candidate for developing citrus canker immunoassays.

Table 2
Kinetic and equilibrium constants for CPXaC obtained from QCM analysis.

Method	k_a (L mol^{-1} s^{-1})	k_d (s^{-1})	K_a (L mol^{-1})
Method I	–	–	$1.6 \pm 0.2 \times 10^6$
Method II	$7.8 \pm 0.2 \times 10^4$	$2.1 \pm 0.3 \times 10^{-2}$	$3.6 \pm 0.3 \times 10^6$

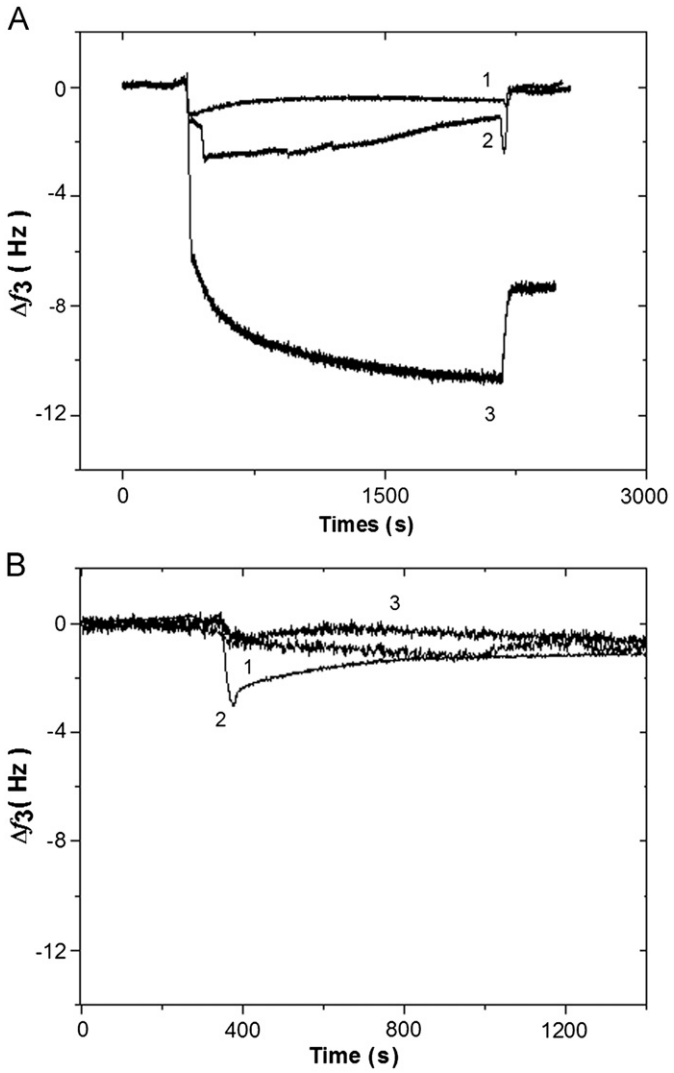

Fig. 4. (A) Real-time frequency variation when (curves 1 and 2) 32 and 64.5×10^{-8} mol L^{-1} CPXaC were injected into the cell with crystal modified without antibody, and (curve 3) 32×10^{-8} mol L^{-1} CPXaC added into the cell with piezoelectric crystal modified with attached antibody. (B) (curve 1) addition of 4.15×10^{-6} mol L^{-1} canecystatin and (curve 2) addition of 3.03×10^{-6} mol L^{-1} BSA and (curve 3) addition of 32.0×10^{-8} mol L^{-1} of *X. fastidiosa* cysteine peptidase to a crystal with immobilized anti-CPXaC.

3.4. Specificity study

The immunosensor specificity was evaluated by modifying the gold surface using procedure IP1 but without the addition of antibody. Only the blocked skim milk solution was added and then exposed to a CPXaC solution in concentrations of 32.0 and 64.5×10^{-8} mol L^{-1}. Fig. 4(A) shows frequency shift when CPXaC was injected to a crystal without anti-CPXaC (curves 1 and 2) and with immobilized anti-CPXaC (curve 3). In the absence of anti-CPXaC, a shift in frequency was observed when CPXaC was added; however after it was washed with PBS buffer, the frequency returned to the initial values, indicating non-specific binding. The specificity of the sensor was checked against different proteins, such as canecystatin [22], BSA, and a cysteine peptidase that is a target for the detection of *Xylella fastidiosa*, a gram-negative bacterium responsible for citrus variegated chlorosis (CVC), which is another important citrus disease [23]. The sensors were exposed to solutions of 4.15×10^{-6} mol L^{-1} of canecystatin or 3.03×10^{-6} mol L^{-1} of BSA or 32.0×10^{-8} mol L^{-1} of *X. fastidiosa* cysteine peptidase, the results are in Fig. 4(B). As can be seen, no detectable signal was observed for the non-target proteins indicating that developed piezoelectric sensor had good selectivity and specificity for CPXaC from *Xcc*.

4. Conclusions

We have presented the development of a piezoelectric immunosensor for CPXaC detection using anti-CPXaC, produced in rabbits, immobilized on a gold crystal surface. The CPXaC-anti-CPXaC interaction studies showed good values for kinetic and affinity constants. The immunosensor showed stable and biocompatible selective interface with non-specific binding with good limit of detection for CPXaC. Therefore, these studies provide new perspectives for using CPXaC as a potential biomarker for highly sensitive piezoelectric immunosensor for citrus canker detection.

Acknowledgments

This work was supported financially by FAPESP (São Paulo Research Foundation) (Proc. no. 08/06867; 11/02259-6), CNPq and CAPES.

Appendix A. Supplementary materials

Supplementary materials associated with this article can be found in the online version at http://dx.doi.org/10.1016/j.talanta.2012.11.003.

References

[1] N.W. Schaad, E. Postnikovaa, G. Lacyb, A. Sechlera, I. Agarkovac, P.E. Stromberga, V.K. Strombergb, A.K. Vidaverc, Syst. Appl. Microbiol. 29 (2006) 690–695.
[2] T.S. Schubert, S.A. Rizvi, X.A. Sun, T.R. Gottwald, J.H. Graham, W.N. Dixon, Plant Dis. 85 (2001) 340–356.
[3] A.K. Das, J. Appl. Hortic. 5 (2003) 52–60.
[4] M. Golmohammadi, J. Cubero, J. Penalver, J.M. Quesada, M.M. Lopez, P. Llop, J. Appl. Microbiol. 103 (2007) 2309–2315.
[5] E.C. Lins, J.J. Belasques, L.G. Marcassa, Precis. Agric. 10 (2009) 319–330.
[6] J. Qin, T.F. Burks, M.A. Ritenour, W.G. Bonn, J. Food Eng. 93 (2009) 183–191.
[7] R.P. Buck, E. Lindner, W. Kutner, G. Inzelt, Pure Appl. Chem. 76 (2004) 1139–1160.
[8] M. Rodahl, F. Höök, A. Krozer, P. Brzezinski, B. Kasemo, Rev. Sci. Instrum. 66 (1995) 3924–3930.
[9] A.M. Saraiva, M.C. Pereira, G. Brezesinski, Langmuir 26 (2010) 12060–12067.
[10] Q. Chen, W. Tang, D.Z. Wang, X.J. Wu, N. Li, F. Liu, Biosens. Bioelectron. 26 (2010) 575–579.
[11] N.C. Pesquero, M.M. Pedroso, A.M. Watanabe, M.H.S. Goldman, R.C. Faria, M.C. Roque-Barreira, P.R. Bueno, Biosens. Bioelectron. 26 (2010) 36–42.
[12] C. Poitras, N. Tufenkji, Biosens. Bioelectron. 24 (2009) 2137–2142.
[13] S. Kay, S. Hahn, E. Marois, R. Wieduwild, U. Bonas, Plant J. 59 (2009) 859–871.
[14] E. Briand, M. Salmain, J.M. Herry, H. Perrot, C. Compere, C.M. Pradier, Biosens. Bioelectron. 22 (2006) 440–448.
[15] C. Zhou, J.M. Friedt, A. Angelova, K.H. Choi, W. Laureyn, F. Frederix, L.A. Francis, A. Campitelli, Y. Engelborghs, G. Borghs, Langmuir 20 (2004) 5870–5878.
[16] M. Rodahl, F. Hook, C. Fredriksson, C.A. Keller, A. Krozer, P. Brzezinski, M. Voinova, B. Kasemo, Faraday Discuss. 107 (1997) 229–246.
[17] F. Hook, M. Rodahl, P. Brzezinski, B. Kasemo, Langmuir 14 (1998) 729–734.
[18] G.Z. Sauerbrey, Z. Phys. 155 (1959) 206–222.
[19] M.M. Pedroso, A.M. Watanabe, M.C. Roque-Barreira, P.R. Bueno, R.C. Faria, Microchem. J. 89 (2008) 153–158.
[20] R.W. Glaser, G. Hausdorf, J. Immunol. Methods 189 (1996) 1–14.
[21] C. Albrechta, P. Fechnera, D. Honcharenkob, L. Baltzerb, G. Gauglitza, Biosens. Bioelectron. 25 (2010) 2302–2308.
[22] A. Soares-Costa, L.M. Beltramini, O.H. Thiemann, F. Henrique-Silva, Biochem. Biophys. Res. Commun. 296 (2002) 1194–1199.
[23] V. Nogaroto, S.A. Tagliavini, A. Gianotti, A. Mikawa, N.M.T. Barros, L. Puzer, A.K. Carmona, P.I. Costa, F. Henrique-Silva, FEMS Microbiol. Lett. 261 (2006) 187–193.